RESEARCH ARTICLE

Bioactive potential of secondary metabolites of rhizospheric fungus *Penicillium citrinum isolate-ABRF3*

Mahendra Kumar Sahu [1]
Digvijay Singh [2, 3]
Sharmistha Chaitali Ghosh [1]
Shruthi Suthakaran [2, 3]
Amitava Das [2, 3]
Harit Jha [1]

Authors' addresses:
[1] Department of Biotechnology, Guru Ghasidas Vishwavidyalaya, Bilaspur – 495009, Chhattisgarh, India
[2] Department of Applied Biology, CSIR-Indian Institute of Chemical Technology, Uppal Road, Tarnaka, Hyderabad – 500 007, TS, India
[3] Academy of Scientific and Innovative Research (AcSIR), Ghaziabad, UP – 201 002, India

Correspondence:
Harit Jha
Department of Biotechnology, Guru Ghasidas Vishwavidyalaya, Bilaspur-495009, Chhattisgarh, India
Tel.: +91 9826630805
e-mail harit74@yahoo.co.in

Article info:
Received: 26 September 2021
*Accepted:*14 January 2022

ABSTRACT

A strain of *Penicillium citrinum* isolate-*ABRF3* collected from the Achanakmar Biosphere, India, was examined for its bioactive potential. Under optimized conditions, secondary metabolites were extracted from the fungus using the solvent extraction method, and all fractions were assessed for antioxidant, antimicrobial, anti-aging, and antiproliferative activity. The highest antioxidant activity was shown by *Penicillium citrinum* ethanolic extract, i.e., 80%, 79%, 77%, and 75% when assessed by 2,2-diphenyl 1-picrylhydrazyl, Ferric reducing power, Phosphomolybdenum, and 2, 2'-azino-bis3-ethylbenzthiazoline-6-sulfonic assays, respectively. A maximum inhibition zone of 17.18 ± 1.3 mm was observed against pathogenic bacteria *Staphylococcus aureus* in the ethyl acetate column fraction compared with standard antibiotics. Ethyl acetate column fraction demonstrated meaningful anti-aging activity against Yeast mutant strain, BY4742, along with methanol and chloroform column fraction depicted a substantial DNA fragmentation and antiproliferative action against a set of mammalian cancer cell lines. The Gas Chromatography with Mass Spectroscopy and Nuclear Magnetic Resonance analysis identified (E)-9-Octadecenoic acid ethyl ester as a significant secondary metabolite in the extract. *In silico* molecular docking was performed for identified metabolite (E)-9-Octadecenoic acid ethyl ester to ascertain its putative role in extract bioactivity, with various anti-aging and anticancer targets.

Key words: *Penicillium*, secondary metabolite, antioxidant, anti-proliferative, anti-aging

Introduction

Fungi are one of the significant sources of a variety of valuable natural products including, novel antibiotics (Davies & Davies, 2010). Some of the antibiotics identified from fungal derivation include griseofulvin obtained from *Penicillium griseofulvum* (Zhou et al., 2010) and cephalosporin from *Cephalosporium* sp. (Martín et al., 2005). Fungi are also an unlimited source of therapeutically beneficial biologically active molecules that have been identified as antitumor, antiviral, anti-inflammatory agents (Maritim et al., 2003). Secondary metabolites with therapeutic potential like antimicrobial, patulin (Demain & Fang, 2000), antioxidant kojic acid (Pandit et al., 2018), anti-inflammatory astaxanthin (Barredo et al., 2017), anticancer 2-morpholinoethylester (Miranda et al., 2010), immunomodulatory drug cyclosporine-A (Hunt et al., 2010) cholesterol-lowering drug (Otto et al., 1995), anticoagulants like tacrolimus (Niwa et al., 2003), antifungal (Claydon et al., 1987) and antiviral compounds have been isolated from fungi (Nishihara et al., 2000). A therapeutic application like increased hypoxia tolerance by *Cordycepssinensis* metabolites (Singh et al., 2013) and extract from *Ganoderma lucidum* fungus have shown promising health benefits during the hypoxic conditions (Koganti et al., 2018). Fungal-derived metabolites can control and influence various cellular and metabolic signaling pathways because of pleiotropic activities (Badri et al., 2009). Further, the association of fungi with plant roots known as rhizospheric fungi shows a mutualistic relationship. In the present study, *Penicillium citrinum* isolate-*ABRF3* was collected from untapped terrain of Achanakmar Forest reserve (situated in the mid-region of India) and evaluated for recognition of natural entities with possible therapeutic outcomes applications. The promising potential natural metabolites were extracted from selected strains using suitable solvents. Adsorption column chromatography was used to purify the extract and subsequently tested for antioxidant, antimicrobial and antiproliferative activity.

Materials and Methods

Chemicals required and used reagents

2, 2-diphenyl-1-picrylhydrazyl (DPPH), 2, 2'azinobis (3-ethyl benzthiazoline-6-sulphonic acid) (ABTS+), was procured from HiMedia. Czapek dox agar, Potato dextrose agar, acarbose, and potassium persulfate were purchased from Sigma-Aldrich, USA. Analytical reagent grades of all the reagents and chemicals were used. All the solvents (toluene, chloroform, ethyl acetate, and methanol) used were of high purity.

Isolation and identification of the fungus

Isolation of rhizospheric fungus isolate-*ABRF3* was done from the soil of Achanakmar forest of Bilaspur, Chhattisgarh (Sahu et al., 2020). Microscopic examination was used for the identification of fungal species. Furthermore, gene sequencing of nuclear ribosome internal transcribed spacer (ITS) regions was performed to identify the fungal species. ITS region of fungus was amplified using Polymerase Chain Reaction (PCR) with ITS specific Forward and Reverse primer (Aharwar & Parihar, 2019; Sahu & Jha, 2020). The primers chosen were particular for the ITS region of the fungal strain. These are the degenerate primers that are used explicitly for identification purposes. The phylogenetic tree was constructed using Mega 6 software with the help of obtained PCR amplified ITS sequence. Twenty-eight aligned sequences of fungi were used for building phylogenetic trees by using Mega 6 software.

Experimental microorganisms

Pathogenic strains *Staphylococcus aureus* (MTCC-96 Gram-positive, Cocci), *Bacillus cerculans (*MTCC-7906 Gram-positive, Rods), *Ralstonia eutrophae* (MTCC-2487 Gram-positive, Rhodococcus), and *Bacillus subtilis* (MTCC 441 Gram-positive, Rods) used for examining the antimicrobial potential of fungal extracts, and yeast BY4742 mutant strain (ATCC No. 201389, MTCC-3157) for assessment of anti-aging characteristics were obtained from CSIR-IMTECH, Chandigarh, India. The microorganism and yeast cultures were cultured on Nutrient Agar Medium (NAM), and Potato Dextrose Agar (PDA) slants, respectively by incubating overnight. The mother culture of these strains was maintained in a separate petri plate and was incubated at 4°C for further experimental utilizations.

Screening of fungal strains

Presumably, all the fungal strains were considered original to produce secondary metabolites of therapeutic importance when subjected to growth in the nutrient media. Thus, five nutrient mediums with comparatively divergent properties in their constituent and compositions like Czapek Dox Broth (CDB), Czapek Dox Yeast Broth (CDYB), Malt Extract Broth (MEB), Potato Dextrose Broth (PDB), and Yeast Extract Sucrose Broth (YESB) were screened for the study of growth patterns of fungus in terms of biomass and secondary metabolite yield. For secondary metabolite production, static fermentation was employed, as it was reported to be more effective than constant shaking fermentation (Lin et al., 1976; Wei et al., 1991). The potent strain was placed in the incubator at 25±2 °C for 15 days or until it formed a fungal mat, indicating any fungal strain's complete growth. Subsequently, the culture was harvested and processed to extract secondary metabolites. For the preparation of crude extract, culture media was treated with 1.5% Tween-80 post-incubation and was subjected to a constant shaker for about 30 min. at an optimum temperature to achieve a homogenous cell wall disruption of the fungal biomass such that intracellular secondary metabolites get released into media. The fungal biomass was filtered to isolate intracellular and extracellular secondary metabolites as described previously with slight modifications (Alkhulaif et al., 2019). The filtrates were collected and concentrated up to 20% of their original volume (v/v) in a vacuum rotary evaporator at 50±5 °C. The residues were further concentrated and stored aptly. The working solution was diluting the stock solution with sterilized distilled water for subsequent analysis.

Identification of optimum nutrient medium

Isolate ABRF3 strain was cultured for 15 days in five different fungal growth mediums to determine the optimal media for growth, development, and production of secondary metabolites. Growth media used in the present study were Potato Dextrose Broth (PDB), Malt Extract Broth (MEB), Czapek Dox Broth (CDB), Yeast Extract Sucrose Broth (YESB), and Czapek Dox Yeast Broth (CDYB) [22]. Maximum growth and production of secondary metabolites were witnessed in the YESB medium when it was incubated at 28 °C for 15 days. The extracts were examined for their antibacterial, antioxidant, anti-aging, and anticancer properties.

Solvent extraction processes

Most of the fungal secondary metabolites were extracted from the dried fungal biomass using the Soxhlet extraction method, which kept ethanol solvent. Crude ethanolic extract was then subjected to column purification with different eluents based on the increasing polarity (non-polar to polar) of solvents, i.e., Toluene, Chloroform, Ethyl acetate, Methanol, and Acetonitrile. As indicated through the preliminary experiments that ethanolic extract showed maximum activity; thus, the ethanolic extract was purified further to obtain a pure compound. The extracted fractions were concentrated and dried under sterilized conditions.

http://www.jbb.uni-plovdiv.bg
DOI: 10.69085/jbb20221001

Thin-layer chromatography (TLC)

The extracts and their various fractions were spotted on silica gel TLC plates. We separated potent compounds through ascending TLC with varying concentrations of mobile phases in the solvent system consisting of acetonitrile: water: acetic acid (18:80:2) (v/v). The plates were air-dried and were observed under the iodine chamber to analyze the movement and TLC profile of metabolites. The fractions with similar TLC profiles were pooled together. The appearance of a single spot in the above TLCs suggested the relative purity of the compounds.

Screening of the crude extract

The antimicrobial and antioxidant activities of the *Penicillium citrinum* isolate-*ABRF3* extract with active secondary metabolite were evaluated by three different methods in triplicates along with respective controls and blanks.

DPPH radical scavenging activity (2, 2-diphenyl 1-picrylhydrazyl)

DPPH radical scavenging activity of extracts was calculated according to previously reported method with modification (Blois, 1958; Dhale & Vijay-Raj, 2009)]. In brief, the reaction was recorded at different time intervals viz. 0 and 30 min for decolorization observation.

FRAP assay (Ferric reducing antioxidant power)

To reveal the antioxidant power of extracts, the FRAP assay was performed (Barapatre et al., 2015). In brief, ionization potential and iron solubility are maintained by low pH drives electron transfer resulting in increased redox potential. Different concentrations of the sample (66.7–166.7µg/mL) were used for evaluating the FRAP activity, which is measured at 595 nm using a spectrophotometer.

ABTS radical cation decolorization assay

Antioxidant ability was performed by the modified 2, 2'-azino-bis3-ethylbenzthiazoline-6-sulfonic (ABTS) method as described previously (Shen et al., 2007). The optical density (OD) was calculated by measuring the UV-Vis spectrometer at 734 nm.

ABTS scavenging activity (%) = (A0 −Ai) /A0×100

Where A0 was the absorbance of the control, and Ai was the absorbance of the sample.

Phosphomolybdenum assay

Antioxidant potential based on the decrease of Phosphate-Molybdenum (VI) to Phosphate-Molybdenum (V) was performed as described earlier (Sahu et al., 2020). OD of the experiment was deliberate at 695 nm. The reducing capacity of extract was calculated by the formula as described earlier (Sowndhararajan & Kang, 2013).

Determination of antimicrobial activity by agar well diffusion method

The antimicrobial activity of the extracts was performed by Agar well diffusion method. Bacterial broth culture was prepared using pathogenic microorganisms as mentioned above. (Balachandran et al., 2016). In the plates, wells of 6 mm diameter were made using a well-borer. In brief, the test is performed by applying a pathogenic bacteria inoculum size 2×10^8 CFU/ml on an agar plate. The column fractionated fractions (50 µl) of different solvents were loaded in wells. Streptomycin (1 mg/mL) served as a positive control and ethanol as vehicle control (Jain et al. 2020). Subsequently, plates were incubated at 37°C for 24 h. The diameter of the zones of inhibition around each of the wells was taken to measure the antibacterial activity**.**

Ethanolic extract purification

The ethanolic extract was purified to get potential natural products, performing column chromatography with silica gel mesh size 60-120. In short, 1 g of fungus crude dissolved in ethanol (1:1 w/v) was loaded on the column. Increasingly polar solvents were used for elution. Every fraction was collected and spectrophotometrically evaluated**.**

Structural identification of the compound

High-performance liquid chromatography (HPLC) analysis

Fungal crude was mixed with the solvent (1:1 w/v) ethanol. The metabolite was determined by HPLC (Shimadzu Liquid Chromatography LC10A) with the help of the C18 analytical column. The calibration curve was obtained using the standard catechin, and phloroglucinol (200 ppm/10 µl of injection volume) as described previously (Shen et al., 2007).

Fourier Transform Infrared spectroscopy

Functional groups of samples purified by column fractionation were determined as described earlier (Azerang et al., 2019). FTIR spectrums of the fractions were obtained at ambient temperature (RT) using Fourier transform infrared spectrometer. In brief, purified compounds were mixed with KBr to form a pellet. The FTIR band ranges were obtained at a frequency range of 4000-400 cm^{-1}.

Gas chromatography-mass spectroscopy (GC-MS)

GC-MS was used for the quantitative and qualitative study of samples as described previously (Li et al., 2017). The secondary metabolites were determined based on their relative index and NIST standards.

Nuclear Magnetic Resonance

The isolated molecule was analyzed using 1H NMR spectra on Bruker advance III 400 MHz nuclear magnetic resonance spectrometer. Samples were prepared in DMSO. The chemical shift was shown as ppm, which was performed

at VIT, Vellore, India. Standards were used for deciphering the molecular formula and putative structure of the compound of interest as described previously (Sharma et al., 2016).

In silico studies

(E)-9-Octadecenoic acid ethyl ester, the isolated and characterized novel fungal metabolite, was subjected to molecular docking along with standard antiaging and anticancer drugs. The energy, mode, scoring functions, binding affinity was calculated against the selected target proteins.

Molecular Docking

PDB or Protein Database provided the structure of target proteins. *moe.2008* (Molecular Operating Environment, 2008) software was used to carry out *in silico* docking study and derive ligand-receptor interactions (Naik et al., 2011). RCSB PDB ID: 2KM1, i.e., Yeast protein Dre2 (Soler et al., 2012); RCSB PDB ID: 1AH8, i.e., chaperone Hsp90 present in N-terminal domain in Yeast (Huai et al., 2005); and RCSB PDB ID: 2L7E, i.e., Yeast Taf14 (Schulze et al., 2010) were selected as the target proteins for antiaging analysis through Molecular Docking. Human antiaging targets RCSB PDB ID: 1US7, i.e., Complex of Hsp90 and P50 chaperon (Roe et al., 2004), RCSB PDB ID: 4ZZH, i.e., SIRT1/Activator Complex (Dai et al., 2015) and RCSB PDB ID: 5UGW, i.e., human telomerase thumb domain (Skordalakes & Hoffman, 2017), were chosen as the target for the antiaging study. Correspondingly, RCSB PDB ID: 3SSU part of the cytoskeletal structure of metazoan cells generally in MDA-MB-231 (Chernyatina et al., 2012); RCSB PDB ID: 6AU4, i.e., human prostate cancer cell line *DU-145* containing c-MYC promoter (Luoto et al., 2010); RCSB PDB ID: 1ELK (Misra et al., 2000); and RCSB PDB ID: 1MP8, i.e., FAK (Focal Adhesion Kinase) (VM, 2010) were chosen as potential anticancer targets for docking related investigations.

Bioactive properties of the isolated compound

Antiaging analysis

To assess the antiaging proclivity of the identified compound, we modified the classical spot assay according to our requirement. We carried out the assay for aging studies using *Saccharomyces cerevisiae* BY4742 [ATCC: 201389 & MTCC: 3157] (Zhao et al., 2017). To demonstrate the modifications, we implemented during this experiment, we discuss each step we followed for this assay. A single cell colony of *S. cerevisiae* BY4742 was inoculated in Yeast peptone dextrose (YPD) broth and then was incubated overnight in a shaking incubator at 28 ± 2ºC. The cultured cells were introduced into fresh YPD media in the ratio 1:1 (50mL inoculum in 50 mL YPD) and subjected for growth till the exponential phase. The cells were separated from the media by centrifuging at 5000g for 10 min, at 20ºC. Next, we washed the cells with 1 M sorbitol (HIMEDIA-PCT0606), and re-suspended them in 1×PBS of pH 7.4 (HiMedia, Mumbai, India). The seed culture for spot assay was diluted to 0.1 until an optical density of 600 nm was obtained. YPD agar plates were prepared, and wells were bored using a sterilized well borer. The potent column fraction (40 µl) was mixed with 10 µl PBS containing cells; it was then introduced into the well as a spot. Nystatin (Fluconazole) was taken as a negative control, whereas acarbose, rapamycin, and culture without any extract were positive controls. Plates were incubated for 72 h at 28 ± 2ºC. Comparative analysis of the fungal metabolite's growth zone with the controls may reveal the antiaging capacities.

Anticancer potential

We assessed the anticancer potential of fungal extracts using different cancer cell lines; *MCF-7*, *MDA-MB-231*, and *MDA-MB-468* (Breast cancer), *A-549* (Lung cancer), *DU-145* (Prostate cancer), *HepG2* (Liver cancer), and *HEK-293* (Primary control cell line) by using SRB assay (Manupati et al., 2019). In brief, a density of 5×10^3 cells per well was seeded in a 96-well plate. Subsequently, cells were treated after 24 h of incubation, with increasing concentration (0.01, 0.1, 1, 10, and 100 mg/mL) of all the fungal extracts prepared in various solvents viz. Water, Methanol, Chloroform, Toluene, Ethyl acetate, and Acetonitrile or respective vehicle controls for two days followed by fixation and SRB staining of treated cells, and absorbance was measured at 510 nm. The percent inhibition (IC50) was calculated using GraphPad Prism (Manupati et al., 2017).

DNA Fragmentation Assay as a confirmatory test

To evaluate the apoptotic effect of the extracts, *MDA-MB-468* cells were treated with the various fractions of the fungal extract isolate-*ABRF3* (10 mg/mL) for 48 h and evaluated for the integrity of DNA post-treatment. Briefly, the TNBC *MDA-MB-468* cells were seeded at a density of 0.5×10^6 cells in Dulbecco's Minimum Essential Medium (DMEM). After 24 h, the cells were treated for 48 h with the extracts (10mg/mL) or positive control Doxorubicin (1 µM). The supernatant was then centrifuged at 2000 rpm to collect the apoptotic cells, and DNA was extracted using standard DNA extraction protocol. The collected cells were incubated overnight with 500 µL of DNA extraction buffer (100 mM NaCl, 10 mM Tris, 25mM EDTA 0.5% SDS, pH 8.0) and proteinase K (0.1 mg/mL) at 55˚C. The cells were then centrifuged to remove cellular debris. The supernatant was mixed with an equal volume of Phenol:Chloroform:Isoamyl alcohol (25:24:1) reagent (Puregene, New Delhi, India). The resultant mixture was then centrifuged at 10000 rpm × 15 min. The supernatant was collected and mixed gently with an equal volume of Chloroform:Isoamyl alcohol (24:1) mixture and centrifuged at 1000 rpm × 15 min. The aqueous phase was then collected, followed by incubation with 1/10th volume Sodium Acetate (3

http://www.jbb.uni-plovdiv.bg
DOI: 10.69085/jbb20221001

M) and twice the volume of isopropanol on ice to pellet the DNA. The pelleted DNA was then washed with 70% ethanol. The resultant pellet was air-dried and dissolved in the desired volume of TE buffer. Total DNA concentration was then quantified using a NanoDrop-1000 spectrophotometer (NanoDrop, Wilmington, USA). 1µg of DNA was then loaded in 0.8% agarose gel and electrophoresed. The gel was then examined for DNA fragmentation (Matassov et al., 2004).

Statistical analysis

Information is presented as the mean ± standard deviation (SD, n = 3). One-way analysis of variance (ANOVA) followed by Duncan multiple range tests was used to find significant variation among different groups.

Results

Isolation and identification

We isolated and characterized the bioactive secondary metabolites from *Penicillium citrinum* isolate-*ABRF3*. The brown crude extracts (Figure SF1A) obtained from the *Penicillium citrinum* isolate-*ABRF3* were screened for antioxidant and antimicrobial activity. The ethanolic crude extract was analyzed to optimize the production of secondary metabolites for the antioxidant activity to detect the reactive oxygen species generated in different nutrient media used for the same fungus. The fungal-derived bioactive metabolite was identified using biophysical techniques such as GC-MS (Gas chromatography coupled with Mass spectrometry) and NMR (Nuclear magnetic resonance), the structure of the molecule was further deciphered using the standard Mass spectrometry databases (Figure SF1B). ABRF3 isolate was distinguished microscopically by cotton blue staining (Figure 1A-B) and bright-field microscopy (Figure 1C). Soluble yellow pigments produced by colonies in the nutrient media were visible by naked eyes (Figure 1A-B). Molecular characterization of the fungus achieved by sequencing the amplicon was deposited to NCBI (Accession number: MK0271338). The sequence similarity index was evaluated by the BLASTN feature of NCBI and prepared the phylogenetic tree (Figure 1D). The amplified sequence showed maximum similarity with *Penicillium citrinum*.

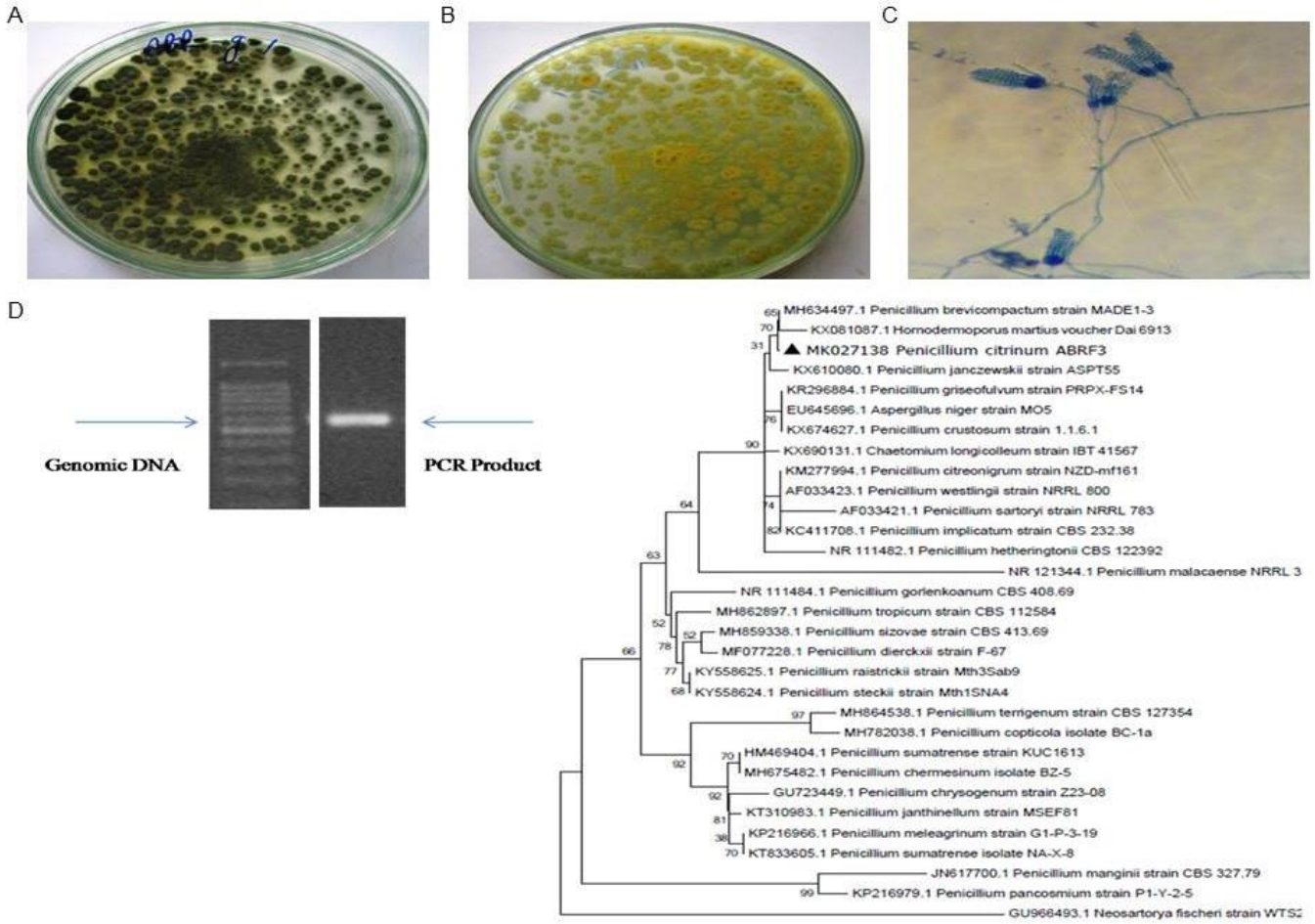

Figure 1. *Isolated fungal strain Penicillium citrinum and their comparative study with morphologically and microscopically. (A) Front view of Penicillium citrinum. (B) Back view of Penicillium citrinum. (C) Microscopic view of Penicillium citrinum. (D) PCR products of isolated fungal strain and Phylogenetic tree of the fungal ITS region from ABRF3 (Penicillium citrinum).*

Screening of the crude extract with the help of antioxidant and antimicrobial assay

Antioxidant activity

Antioxidant activity of the various crude ethanolic extract was determined using various different methods. We observed that the YESB crude extract has more scavenging power to reduce the reactive oxygen species (ROS) compared with other mediums of crude extract (Figure 2). The percent scavenging activity of YESB crude was obtained highest at 77%, 79%, 75%, and 80% as assessed by FRAP radical, DPPH, ABTS, and PM assay, respectively.

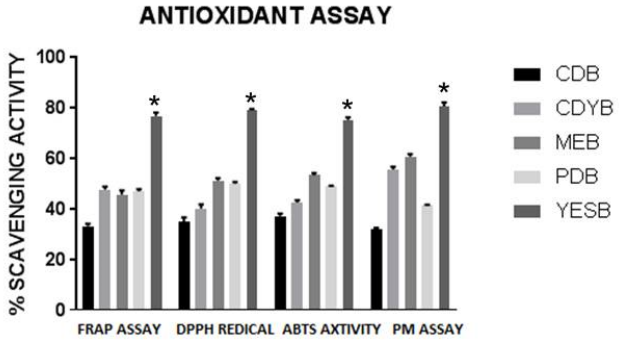

Figure 2. *Antioxidant activity of crude extract of secondary metabolites of isolate ABRF3 (Penicillium citrinum). Data are represented as mean±SD; CzapekDox yeast broth - CDYB, CzapekDox broth - CDB, Malt extract broth–MEB, Potato dextrose broth (PDB), Yeast extract sucrose broth – YSEB and control- positive control (Ascorbic acid). One way ANOVA was applied. The sample with p <0.05 were considered significant.* $^{*}p < 0.05$ *and* $\neq p < 0.01$.

Antibacterial activity

Relatively pure compound acquired by column chromatography was investigated for antibacterial properties with a concentration gradient. Fungal extract suppressed the growth of gram-positive and gram-negative bacteria viz. *S. aureus*, *B. cerculans*, *B. subtilis*, and *Ralstonia eutropha* at a high concentration of 100µg/mL (Figure 3 and Table S1).

Characterization and purification of the active metabolite.

Secondary metabolites assessment using TLC

The effective crude ethanolic extract of isolate *ABRF3* and fractions from column purification was mottled on the TLC sheet made up of silica gel. Thin-layer chromatography (TLC) was employed to separate components detected by UV Illumination. Crude sample (spot A) and chromatography fractionate of ethyl acetate and acetonitrile extract gave light spots under UV Illuminator (Spot B and C) on TLC separation. Spot A, B, and C gave Rf values 0.751, 0.61, and 0.53, respectively (Figure SF2).

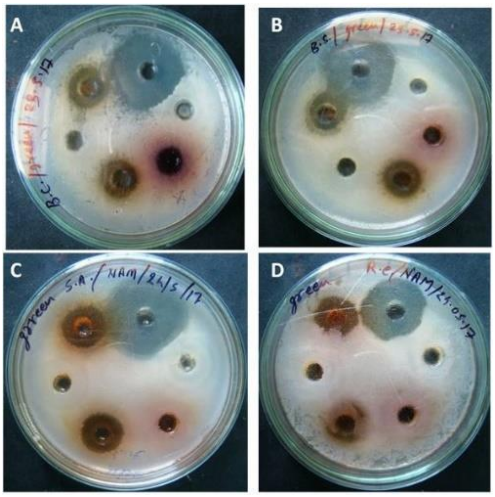

Figure 3. *Antimicrobial activity with zone of inhibition of natural products of isolate ABRF3 (Penicillium citrinum) against pathogenic bacterial and fungal strain. (A) Column fractions against Bacillus circulans, (B) Column fractions against Bacillus subtilis, (C) Column fractions against S. aureus, and (D) Column fractions against R. eutrophae.*

Secondary metabolites evaluation using HPLC

HPLC analysis of the selected *Penicillium citrinum* showed various peaks in the spectrum (Figure 4A). Rf determined values as 2.1667, 2.6, 2.8667, 3.0833, 3.4333, 3.95, 4.55, 4.6667, 5, and 9.3167 for the observed peaks (Table S2).

GC-MS analysis of the compound isolated from ABRF3

Purified fractions of the screened sample exhibited the manifestation of seven peaks (Figure 4B). Secondary metabolites consistent with these peaks were resolved as depicted in Table S3. (E)-9-Octadecenoic acid ethyl ester, (Highest molecular weight 310 Da) (Figure 4C) one of the metabolites was selected for evaluating its potential therapeutic application as others detected were either primary metabolites or solvents that lack biological activity (Table S3).

FTIR analysis of relatively pure compounds

The Ethyl Acetate fraction (EAF) and Acetonitrile fraction (ANF) of *Penicillium citrinum* isolate-*ABRF3* showed a broad range of absorption (3260- 1412cm-1) during FTIR analysis because of the presence of hydroxyl group in phenolic as well as aliphatic compounds which stretched or oscillated the -OH group (Figure 5A-B). At 1188 cm-1, a distinctive peak in the ethyl acetate fraction was identified, representing C–OH, and C-C stretching due to esters. Absorption at 1458.25 and 1412.92 indicated COO- symmetric stretching, whereas absorption observed at 2929.03 cm-1 in ethyl acetate fraction indicated alkane and amine group stretching (Table S4).

http://www.jbb.uni-plovdiv.bg
DOI: 10.69085/jbb20221001

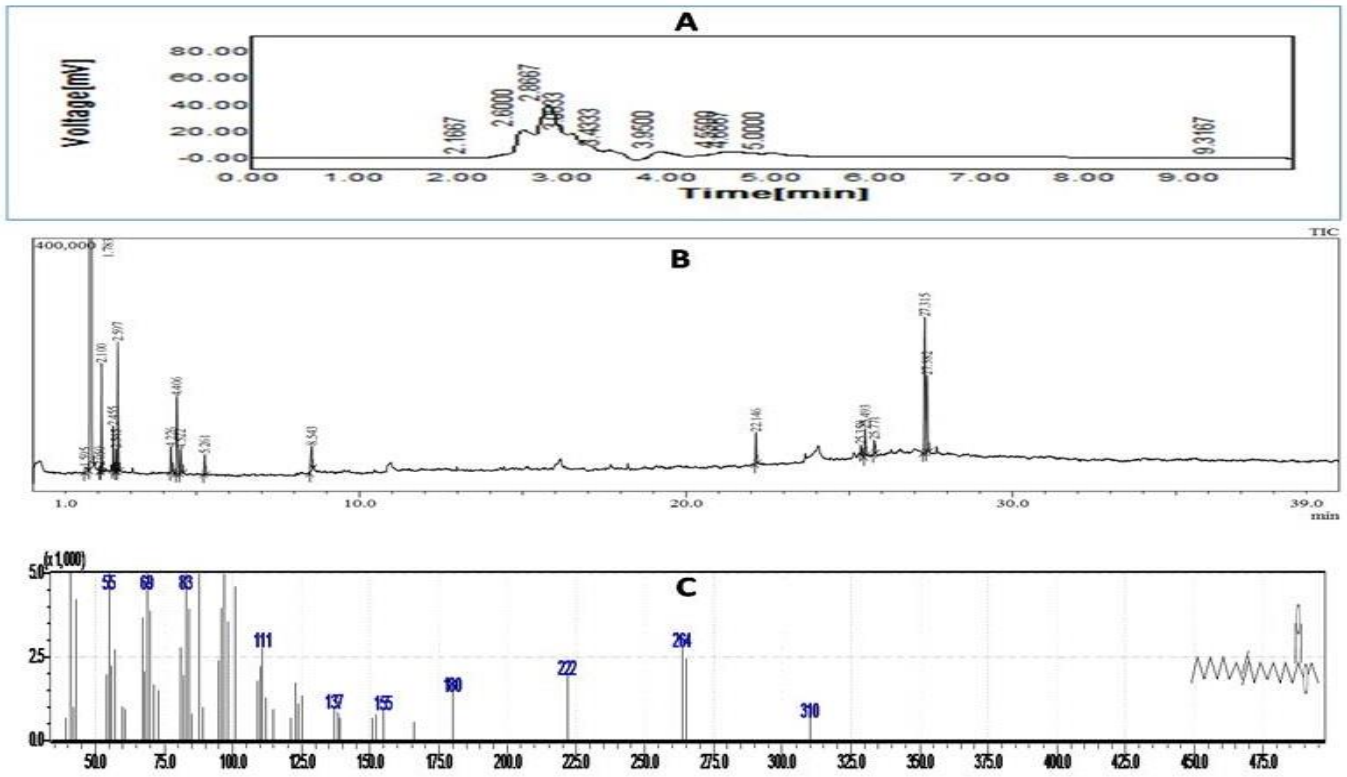

Figure 4. *Chromatographic and spectroscopic analysis of the purified compounds. (A) Purification of secondary metabolites by using HPLC, (B) Depicted graph is GC-MS Analysis of natural products of isolate ABRF3 (Penicillium citrinum), and (C) Depicted the molecular weight of the compound i.e. molecular weight 310 Da of (E)-9-Octadecenoic acid ethyl ester.*

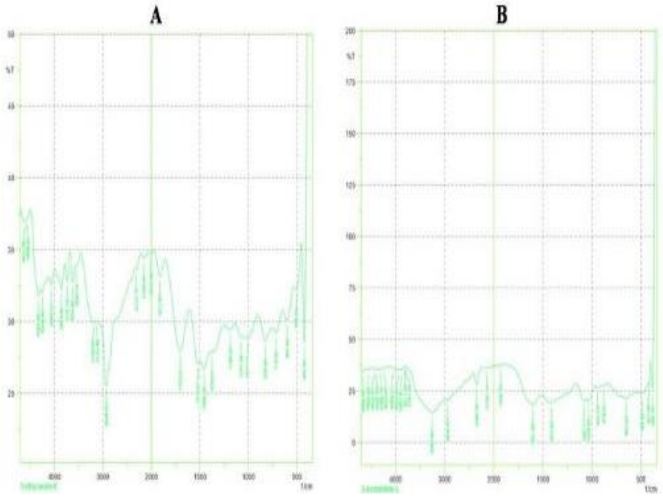

Figure 5. *FTIR Analysis of the column fraction of isolate ABRF3 (Penicillium citrinum). (A) Graph represents the FTIR pattern of ethyl acetate fraction of column fraction, (B) Graph represents the FTIR pattern of acetonitrile fraction of column fraction.*

The existence of an aromatic ring replacing the ester bond was reflected by the spectrum of IR, thus clearly suggesting the predictable functional group of the molecule present in the ethyl acetate column fraction.

[1]HNMR

EAF Column fraction was subjected to structural characterization using the NMR spectrum, and the peaks were observed at a mixture of į values of proton 1H (Figure 6). As predicted from the data values, the antibacterial compound contains methyl, hydroxyl, and ketone groups. [1]H NMR spectra exhibited a plausible antimicrobial molecule with functional groups such as CH2, CH3, OH, and C-H protons. Furthermore, primary data of the compound displayed the occurrence of the C, H, and -OH group, which indicates the presence of ester.

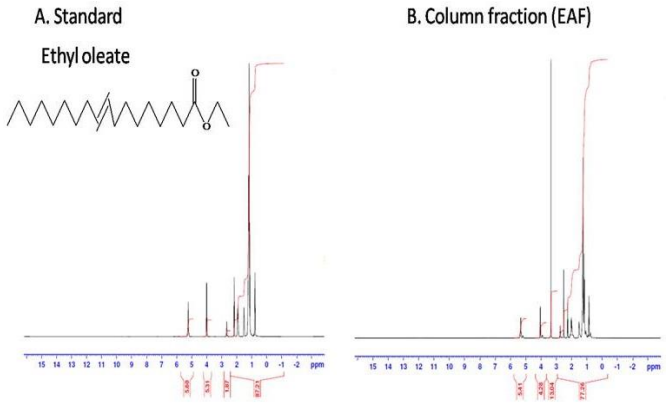

Figure 6. *NMR spectrum of column fraction of Penicillium citrinum isolate-ABRF3 as compared with standard.*

Table 1. *In silico therapeutic studies of the compound with different targets in respect of binding energy and number of direct contacts (all polar, non-polar interactions).*

Compound name	Therapeutic studies	Max affinity with site	Binding energy (kCal/mol)	No. of direct contacts (all polar, non-polar interactions)
(E)-9-Octadecenoic acid ethyl ester with 2KM1: protein binding	Antiaging study	Site-8	-11.1234	Leu 63, Phe 73 (direct contacts).
(E)-9-Octadecenoic acid ethyl ester with 2L7E :Transcription		Site-1	-10.4237	Tyr 56, Leu 58, (direct contacts).
(E)-9-Octadecenoic acid ethyl ester with 1AH8		Site-2	-10.0245	Asn 337, Leu 89, (water hydration). Phe B128, Ser B126, Gly B118, Phe B120, (direct contacts).
(E)-9-Octadecenoic acid ethyl ester with 4ZZH	Antiaging study with human targets	Site1	-10.9107	Asn 417, Phe 297, Lys 408, His 363, Glu 410, Ile 299, Pro 409, Ser 365 (direct contacts).
(E)-9-Octadecenoic acid ethyl ester with 1US7		Site 2	-10.6175	Gly A83, Ile A167 (water hydration). Lys A139, Ser A138, Ile A137, Arg A174, Ile A77, Asp A79 (direct contacts).
(E)-9-Octadecenoic acid ethyl ester with 5UGW		Site 11	-10.3405	Arg 972 (water hydration). Met 970, Gly 967 (direct contacts).
(E)-9-Octadecenoic acid ethyl ester with 6AU4: DNA	Anticancer study	Site-4	-10.7816	DT A16, DA A21, DG A4, DA B22, DG A14, DG A5, DG A13 DG A9, DG A5, DG A8, DG A15, DG A6, DG A10 (direct contacts).
(E)-9-Octadecenoic acid ethyl ester with 1MP8 :Transferase		Site-2	-11.2795	Glu 506, Glu 430, Asp 564, Lys 454, Phe 433 (water hydration). Gln 432, Gly 431, Cys 502, Ile 428 (direct contact).
(E)-9-Octadecenoic acid ethyl ester with 3SSU		Site-1	-8.1199	Glu A187, Asp A181, Arg A184, (direct contact).
(E)-9-Octadecenoic acid ethyl ester with 1ELK		Site-1	-11.8709	DG A14, DG A13, DT A11, DG A15, DG A17, DG A18, DG A4, DG A19, DA B22.

It depicted the presence of a broad peak at 0.8, 1.3, and 1.6δ, which are primary, secondary, and tertiary aliphatic clusters, respectively (Figure 6). The selected and isolated compound was identified as (E)-9-Octadecenoic acid ethyl ester (ethyl oleate) (Table S5).

Functional characterization of the compound

Anti-aging property

Estimation of anti-aging perspective by molecular docking

We performed *in silico* molecular docking analysis to determine the binding of the target protein receptors with the compound of interest and investigate the significant amino acid hotspots in the active site of the targets to reveal efficient chemical bonding and its mode of interactions. The goal was to assess active metabolites' putative interaction and activity against selected anticancer and anti-aging targets.

Docking of (E)-9-Octadecenoic acid ethyl ester against selected anti-aging targets was undertaken using moe.2008. (E)-9-Octadecenoic acid ethyl ester was observed to be compatible with eukaryotic cell growth that was validated using yeast, thereby suggesting (E)-9-Octadecenoic acid ethyl ester as a potent anti-aging compound (Table 1 and S6).

The binding energy or –▲G value for target 1AH8 and (E)-9-Octadecenoic acid ethyl ester was observed to be -10.0245 Kcal/mol. The amino acid hotspots of 1AH8 present in the active site or the binding pocket that directly forms contact are Phe B128, Ser B126, Gly B118, and Phe B120. (E)-9-Octadecenoic acid ethyl ester was observed to interact with Asn 337 and Leu89 by forming two hydrogen bonds (Binding energy -10.0245 kCal/mol) (Figure 7A).

The binding energy or –▲G value for target 2KM1 or Yeast protein Dre2 was -11.1234 (Site 8), which was better than the control drug Sirolimus. (E)-9-Octadecenoic acid ethyl ester depicted a direct interaction with two amino acids, Leu 63 and Phe 73 (Figure 7B).

The binding energy or –▲G value for target 2L7E or Taf14 containing YEATS domain at N-terminus was observed to be -10.4237 Kcal/mol. A direct interaction between the purified secondary metabolite and amino acids Tyr 56 and Leu 58 was observed (Figure 7C).

http://www.jbb.uni-plovdiv.bg
DOI: 10.69085/jbb20221001

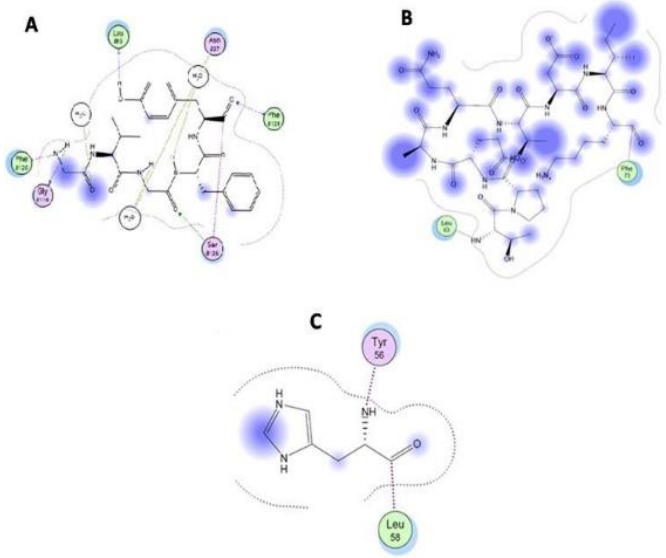

Figure 7. *2D diagram of the Molecular docking of the compound (E)-9-Octadecenoic acid ethyl ester showing its interaction with anti-aging targets active site. (Distance in Å). (A) 2D diagram of 1AH8 residues interacting with compound (E)-9-Octadecenoic acid ethyl ester forming polar contacts with the ligands and residues showing in lines participating in other interactions. (B) 2D diagram of 2KM1: protein binding interacting with compound (E)-9-Octadecenoic acid ethyl ester. (C) 2L7E: Transcription interacting with compound (E)-9-Octadecenoic acid ethyl ester.*

In vitro determination of anti-aging potential

To experimentally evaluate the anti-aging property of the isolate, yeast spot assay and biomass growth determination were implemented using the simplest yet dynamic yeast BY4742, a mutant strain designed for aging-related studies (ATCC No. 201389 and MTCC No. 3157) (Wei et al., 2017).

Nystatin, an ionophore that binds to ergosterol, a portion of fungal plasma membrane marking outflow of potassium ions thereby decreasing the pH of a cell (acidification) destroying fungal cell; was selected as a negative control. Acarbose, an alpha-glucosidase inhibitor, and Rapamycin, an anti-proliferative drug acts by dephosphorylation of S6K1 essential for protein synthesis, were chosen as positive controls for anti-aging and anticancer drugs, respectively. The concentration of each of these controls was kept at 1mg/ml for trials. The culture with EAF column fraction exhibited a spot diameter of 13 ± 1.2 mm, more than culture without EAF fraction albeit less than positive controls acarbose and rapamycin (Figure 8A; Table S7). The level of yeast growth exhibited on the plate in the presence of the compound/drugs was considered an anti-aging effect of the selected fraction.

Negative control, Nystatin demonstrated no growth. The anti-aging activity was further authenticated by an additional

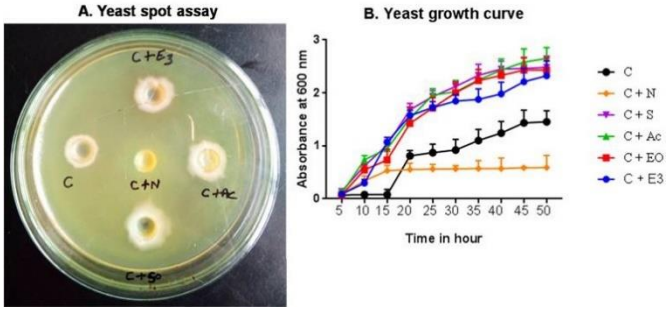

Figure 8. *In vitro spot assay of anti-aging activity of the crude extract of secondary metabolites of isolate ABRF3 (Penicillium citrinum). (A) S. cerevisiae BY4742 cells Spotted onto YPD plates. (B) Growth curve for the S. cerevisiae BY4742 strain were measured in YPD medium. P < 0.05 indicated a significant difference. Fungal extract and their spots generated during Spot Assay along with control systems using S. cerevisiae BY4742. C- Culture only (S. cerevisiae BY4742), C+E3- culture and extract of isolate ABRF3, C+N- culture and Nystatin (negative control), C+Ac- culture and Acarbose, C+ Co- culture and coumarin.*

technique, known as the Yeast Growth curve assay. We observed that the exponential phase was relatively increased in the culture with EAF fraction compared with the positive control, i.e., Acarbose and Rapamycin, and the negative control, Nystatin (Figure 8B).

Anti-proliferative potential analysis

Evaluation of anticancer property using Molecular Docking studies

Molecular docking analysis for anticancer potential was performed using four different targets, i.e., 6AU4, 1MP8, 1ELK, and 3SSU. Doxorubicin is an established antimitotic and cytotoxic agent. Noscapine is also an antimitotic agent, which disrupts the microtubule assembly dynamics (elongation and depolymerization) in the cancer cells (Tomar et al., 2019). Therefore, Doxorubicin and Noscapine were taken as standards for molecular docking experiments of anticancer activity. Results show that E-9-Octadecenoic acid ethyl ester binds to the selected targets through active site amino acids with binding energy –▲G comparable to the positive control and standards (Table S8, Figure 9A-D, Figure SF3).

Anticancer potential of isolates using Sulphorhodamine B assay

The anticancer potential of *Penicillium citrinum* isolate-*ABRF3*, fungal extracts depicted significant cytotoxicity of the methanol fraction against all the cancer cell lines with IC50 ranging from 4=-60 mg/mL. Interestingly, the methanolic fungal extract did not show any inhibition of cell proliferation in primary cells (HEK-293), suggesting a productive cytotoxic agent bearing fraction with relatively low non-specific effects (Table 2).

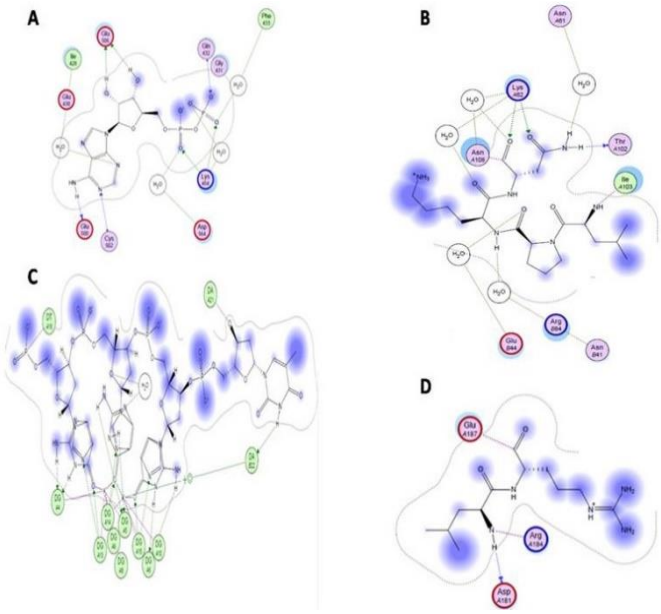

Figure 9. *Molecular docking and 2D interaction diagram showing (E)-9-Octadecenoic acid ethyl ester compound docking pose interaction with the key amino acids in the different anti-cancer cell line targets active site. (Distance in Å). (A) (E)-9-Octadecenoic acid ethyl ester with 1MP8: Transferase. Interact with structure of the cancer related Focal Adhesion Kinase (FAK) and molecule. (B) (E)-9-Octadecenoic acid ethyl ester with 1ELK. Interaction of 1ELK (MCF-7) VSH domain of TOM 1 (target of myb 1) protein from Homo sapiens with molecule. (C) (E)-9-Octadecenoic acid ethyl ester with 6AU4: DNA. Interaction with crystal structure of the major quadruplex formed in the human c-MYC promoter and molecule. (D) (E)-9-Octadecenoic acid ethyl ester with 3SSU. Interaction between Crystal structure of vimentin central helical domain and its implications for intermediate filament assembly 3SSU (MDA MB 231) and obtained molecule.*

Although the toluene fraction of the fungal extracts also depicted no cytotoxicity against the control primary cells, this extract showed a higher concentration of IC50 (40 - 120 mg/mL) against the various cancer cell lines (Table 2). The other solvent fractions of the fungal extracts depicted similar cytotoxicity at higher concentrations of the extracts against the cancer cells and primary cells.

DNA Fragmentation Assay

Activation of nuclear endonuclease during apoptosis leads to fragmentation of DNA that can then be visualized on an agarose gel. Higher molecular weight genomic DNA formed an intense band at the top. DNA fragments were visible as a smear in the case of the methanol, chloroform, ethyl acetate, acetonitrile fractions, and positive control; Doxorubicin treated *MDA-MB-468* cells (Figure 10).

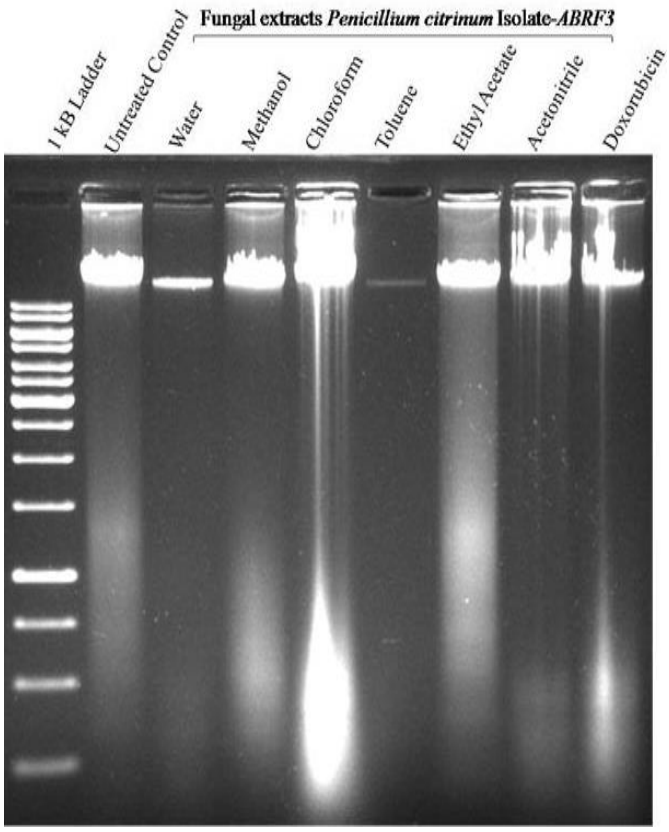

Figure 10. *DNA fragmentation analysis. Methanol, chloroform, ethyl acetate, and acetonitrile fractions of the fungal extract isolate- ABRF3 (10 mg/mL, 48 h) was observed to impart DNA fragmentation in MDA-MB-468 cells. Doxorubicin (1 µM, 48 h) was used as a positive control.*

Proposed cellular pathway for (E)-9-Octadecenoic acid ethyl ester (ethyl oleate)

Mechanism of action for anti-aging activity

In our proposed model, we show that (E)-9-Octadecenoic acid ethyl ester (ethyl oleate) binds with and activates Taf14 essential for the stability of transcription pre-initiation complex yeast, which possibly will result in delayed aging of the yeast. (E)-9-Octadecenoic acid ethyl ester (ethyl oleate) may also act as a scaffold protein for Hsp90 or regulatory activity for the protein kinase (Figure 11A).

Mechanism of action for anticancer activity

Our study identified focal adhesion kinase (FAK) as another target binding partner of ethyl oleate. Moreover, ethyl oleate binds and regulates the functions of Vimentin. We suggest that ethyl oleate interacts with c-myc and control DNA double-strand break (DSB) repair genes expression and thus may be a target candidate for anticancer therapy, thereby leaving cancer cells prone to DNA damage to avert genetic unsteadiness (Figure 11B).

http://www.jbb.uni-plovdiv.bg
DOI: 10.69085/jbb20221001

Table 2. *Assessment of cytotoxic profile of different extracts against various tissue-specific cancer as well as non-cancerous cell lines.*

Fungal extracts *Penicillium citrinum Isolate-ABRF3*	**IC_{50} (mg/mL)[a]**						
	HepG-2[b]	**A-549[c]**	**DU-145[d]**	**MCF-7[e]**	**MDA-MB-231[f]**	**MDA-MB-468[g]**	**HEK-293[h]**
Water	123.91 ± 14.64	16.13 ± 4.36	52.18 ± 1.07	67.04 ± 13.95	59.5 ± 3.21	15.85 ± 2.62	68.1 ± 18.58
Methanol	60.24 ± 29.88	4.34 ± 1.52	29.03 ± 18.26	47.05 ± 4.23	37.74 ± 9.84	10.15 ± 1.58	NI
Chloroform	299.4 ± 76.21	6.83 ± 4.10	28.24 ± 14.04	41.91 ± 6.24	55.32 ± 2.98	39.92 ± 10.64	132.53 ± 31.94
Toluene	81.09 ± 31.53	121 ± 43	27.92 ± 17.63	50.61 ± 6.20	113.43 ± 24.01	40.59 ± 11.71	NI
Ethyl acetate	79.44 ± 14.92	122.82 ± 77.34	52.01 ± 1.77	30.14 ± 7.81	21.93 ± 2.32	48.93 ± 7.93	114.15 ± 80.72
Acetonitrile	69.42 ± 29.35	17.33 ± 10.11	155 ± 53.5	62.74 ± 4.16	8.54 ± 1.59	19.35 ± 5.59	NI
Doxorubicin	5.06 ± 0.72	0.65± 0.15	0.30± 0.06	0.018± 0.007	1.65± 1.55	3.35± 0.54	70.45± 8.12

NI – No inhibition.
[a]50% inhibitory concentrations and mean ± SEM of IC_{50} (mg/mL) values of different fractions represent the mean of three individual experiments.
[b]Liver hepatocellular carcinoma.
[c]Adenocarcinoma human alveolar basal epithelial cells Lung cancer.
[d]Moderate metastatic potential (PSA+) Androgen-independent Prostate cancer.
[e]Luminal-A ($ER^+/PR^+/Her2^-$) Breast cancer.
[f]Basal Triple negative ($ER^-/PR^-/Her2^-$) Breast cancer.
[g]Basal (low claudin) Triple negative ($ER^-/PR^-/Her2^-$) Breast cancer.
[h]Non-cancerous primary human embryonic kidney cells.

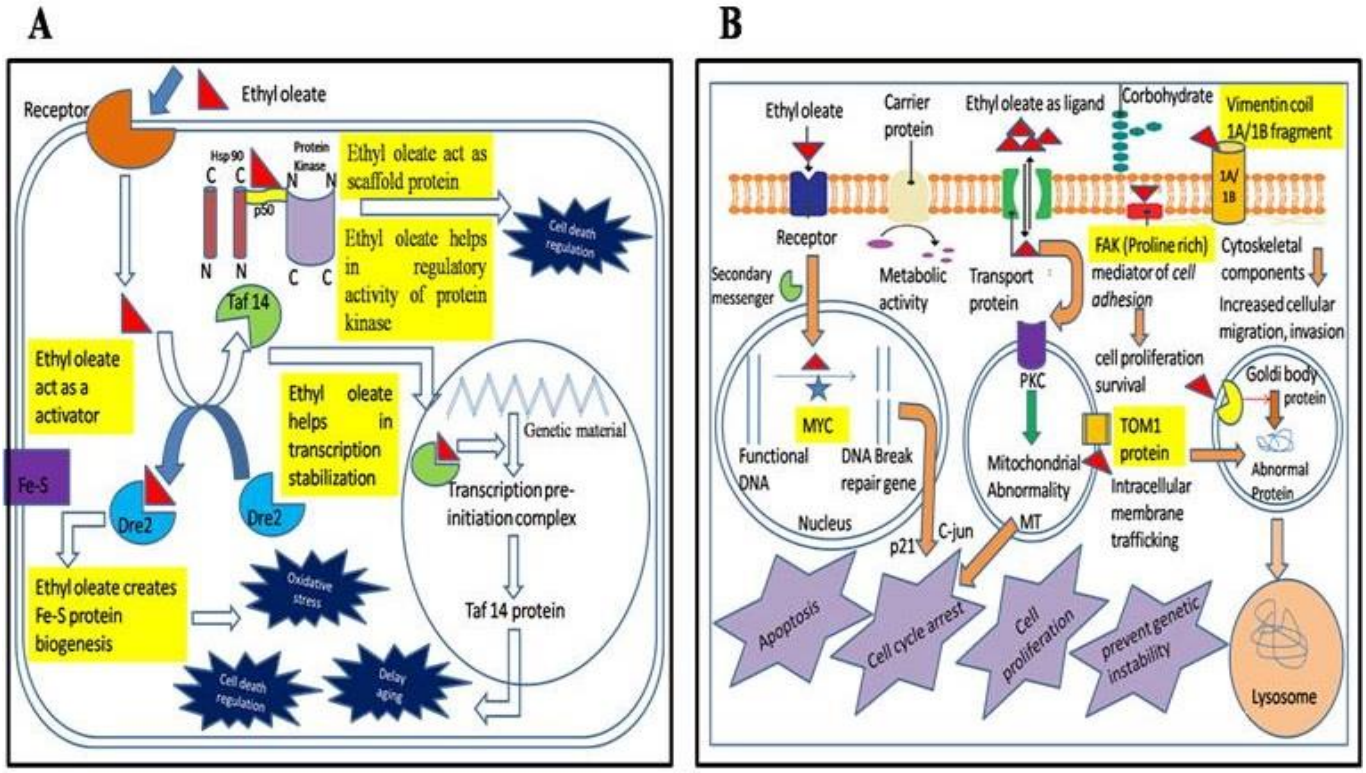

Figure 11. *Proposed cellular pathway and mechanism of action of Ethyl oleate. (A) Mechanism of action of ligand ethyl oleate with antiaging targets. (B) Mechanism of action of ethyl oleate as ligand with targets of anticancer activity.*

Discussion

Penicillium citrinum isolate-*ABRF3* was identified based on the fungus's morphological appearances and sequence similarity. The secondary metabolites present in the intracellular extract of *Penicillium citrinum* isolate-*ABRF3* demonstrated higher bioactivity than extracellular secondary metabolites, and therefore, the extract was accumulated and preserved for further study. These were similar to the antioxidant activity in *Talaromyces purpureogenus* CFRM02 (Pandit et al., 2018). The column-purified fraction of crude extract obtained was subjected to bioactivity assay (Wyatt et al., 2013; Gautier et al., 2016). Column purified fraction containing secondary metabolites was initially evaluated for antimicrobial potential. Ethyl acetate fraction (EAF) and acetonitrile fraction (ANF) from *Penicillium citrinum* isolate-*ABRF3* suppressed Gram-positive and Gram-negative bacteria (Sarker et al., 2007).

The TLC of ethyl acetate fraction revealed three spots with an Rf value between 0.5 to 0.7, which resembles an alternariol-like compound isolated from fungal species (Palanichamy et al., 2018).

In HPLC analysis for identifying active components, two compounds with Rt value 2.8667 and 3.0833 were eluted and found soluble in methanol, ethyl acetate, chloroform, acetone, and ethanol organic solvents, respectively. The fraction subjected to GCMS yielded (E)-9-Octadecenoic acid ethyl ester (highest molecular weight of 310 Da) as one of the identified metabolites as a putative active component selected for further study as esters compounds were earlier reported to demonstrate therapeutic activities, such as antibacterial activities (Zhai et al., 2016). FTIR confirmed the identity of a compound and its structural group. The NMR of ethyl acetate column fraction elucidated esters group at 4.1δ, verifying the presence of an isolated compound in the Ethyl acetate column fraction (Parshikov et al., 2015).

Delayed progression in aging may be correlated to carcinogenesis. Rapamycin and other analogous compounds suppress cellular senescence, slow-down aging progression, and age-linked ailments (Parshikov et al., 2015). Intriguingly, similar signaling molecules are reported to be the targets in cancer therapy (Blagosklonny, 2012). Based on the literature outlined (Wei et al., 2017), we tried to correlate yeast growth and *in silico* data to anti-aging potential propose that the fungal EAF fraction may have metabolite accountable for the improvement of the cell's lifespan.

Our study proposes a cellular pathway for (E)-9-Octadecenoic acid ethyl ester (ethyl oleate) action on anti-aging. To understand the role of ethyl oleate in anti-aging, we selected three specific protein targets (Taf14, Hsp90, and Dre2) of ethyl oleate based on previous findings (Roe et al., 2004; Soler et al., 2012; Sein et al., 2018). Furthermore, our docking studies also indicate that the binding between ethyl oleate and yeast Dre2 (essential Fe-S cluster-containing protein) may be associated with cytosolic Fe-S protein's biogenesis and apoptosis in response to oxidative stress (Soler et al., 2012). The proposed hypothetical model has been illustrated in Figure 11A. To understand the anticancer activity mechanism of ethyl oleate, we selected c-myc as a target that regulates numerous genes governing cell differentiation, proliferation, metabolism, and apoptosis (Luoto et al., 2010). Vimentin has been reported as a potential target used as a marker for epithelial-mesenchymal transition (EMT) (Satelli & Li, 2011). We also found TOM1 protein as one of the targets of ethyl oleate. Recent studies suggest that Tom1, of VHS domain proteins, is a promising candidate as a signaling molecule that has a role in post-Golgi trafficking (Wang et al., 2010). A hypothetical pathway has been proposed for the ethyl oleate action against anticancer targets (Figure11B).

The *in silico* analysis and experimental validation studies suggest significant antioxidant and anti-aging activity of the identified putative active secondary metabolite selected from the fungal extract. The results demonstrated the anti-proliferative activity of ethyl acetate extract and (E)-9-Octadecenoic acid ethyl ester, although observed, was not as comparable to standard drug doxorubicin. The anti-proliferative and anti-aging activity of the extract and metabolites may be attributed to the binding of these molecules with specific targets and their consequent modulation to regulate metabolic and molecular processes and not due to toxic effects.

Conclusion

The *Penicillium citrinum* isolate-*ABRF3* secondary metabolite production and activity were observed under the optimized condition of YESB media and static incubation conditions. Metabolites purified by column chromatography were characterized and assayed for bioactivity. GCMS and NMR performed structural characterization of potent metabolites. (E)-9-Octadecenoic acid ethyl ester (ethyl oleate) was identified as a potent metabolite from *Penicillium citrinum* ethyl acetate fraction. Computer-based docking analysis against anti-proliferative and delayed aging targets represented interaction with standard drugs. The active components identified using *in silico* analysis have been validated utilizing *in vitro* yeast spot assay for anti-aging activity and anti-proliferative activity against various cancer cell lines for anticancer activity. Thus, (E)-9-Octadecenoic acid ethyl ester identified in ethyl acetate extract of *Penicillium citrinum* isolate-*ABRF3* can be a potent molecule for drug development.

http://www.jbb.uni-plovdiv.bg
DOI: 10.69085/jbb20221001

Acknowledgements

This work was supported by the institutional grant and the authors are thankful to the Department of Biotechnology, Guru Ghasidas Vishwavidyalaya for providing the necessary facilities to carry out the research work. The work is also supported by UGC SAP project no. F.3-14/2016/DRS-I (SAP-II) and DBT BUILDER (BT/PR 7020/INF/22/172/2012). AD acknowledges the funding provided by DBT, Government of India, Cancer Pilot Project, and Sanction No. 6242-P65/RGCB/PMD/DBT/AMTD/2015, and CSIR-IICT institutional funding. The fellowship provided by CSIR-JRF/SRF to DS and SS is gratefully acknowledged. (Manuscript Communication Number: IICT/Pubs./2020/211).

References

Aharwar A, Parihar DK. 2019. Talaromyces verruculosus tannase production, characterization and application in fruit juices detannification. Biocatal. Agric. Biotechnol., 18: 101014.

Alkhulaif MM, Awaad AS, AL-Mudhayyif HA, Alothman MR, Alqasoumi SI, Zain SM. 2019. Evaluation of antimicrobial activity of secondary metabolites of fungi isolated from Sultanate Oman soil. Saudi Pharmaceutical Journal, 27: 401-405.

Azerang P, Khalaj V, Kobarfard F, Owlia P, Sardari S, Shahidi S. 2019. Molecular Characterization of a Fungus Producing Membrane Active Metabolite and Analysis of the Produced Secondary Metabolite, Iran Biomed J., 23(2): 121-128.

Badri DV, Weir TL, van der Lelie D, Vivanco JM. 2009. Rhizosphere chemical dialogues: plant-microbe interactions. Curr. Opin. Biotechnol., 20(6): 642-650.

Balachandran C, Duraipandiyan V, Arun Y, Sangeetha B, Emi N, Al-Dhabi NA, Ignacimuthu S, Inaguma Y, Okamoto A, Perumal PT. 2016. Isolation and characterization of 2-hydroxy-9,10-anthraquinone from Streptomyces olivochromogenes (ERINLG-261) with antimicrobial and antiproliferative properties. Rev. bras. Farmacogn., 26(3): 285-295.

Barapatre A, Aadil KR, Tiwary BN, Jha H. 2015. In vitro antioxidant and antidiabetic activities of biomodified lignin from Acacia nilotica wood. International Int. J. Biol. Macromol., 75: 81-89.

Barredo JL, García-Estrada C, Kosalkova K, Barreiro C. 2017. Biosynthesis of Astaxanthin as a Main Carotenoid in the Heterobasidiomycetous Yeast Xanthophyllomyces dendrorhous. Journal of Fungi, 3(3): 44.

Blagosklonny MV. 2012. Rapalogs in cancer prevention: anti-aging or anticancer? Cancer Biol. Ther., 13(14): 1349-1354.

Blois MS. 1958. Antioxidant Determinations by the Use of a Stable Free Radical. Nature, 181:4617, 1199-1200.

Chernyatina AA, Nicolet S, Aebi U, Herrmann H, Strelkov SV. 2012. Atomic structure of the vimentin central α-helical domain and its implications for intermediate filament assembly. PNAS, 109(34): 13620-13625.

Claydon N, Allan M, Hanson JR, Avent AG. 1987. Antifungal alkyl pyrones of Trichoderma harzianum. Trans. Br. Mycol. Soc., 88(4): 503-513.

Dai H, Case AW, Riera TV, Considine T, Lee JE, Hamuro Y, Zhao H, Jiang Y, Sweitzer SM, Pietrak B, Schwartz B, Blum CA, Disch JS, Caldwell R, Szczepankiewicz B, Oalmann C, Yee Ng P, White BH, Casaubon R, Narayan R, Koppetsch K, Bourbonais F, Wu B, Wang J, Qian D, Jiang F, Mao C, Wang M, Hu E, Wu JC, Perni RB, Vlasuk GP, Ellis JL. 2015. Crystallographic structure of a small molecule SIRT1 activator-enzyme complex. Nat Commun., 6: 7645-7645.

Davies J, Davies D. 2010. Origins and Evolution of Antibiotic Resistance. Microbiol. Mol. Biol. Rev., 74(3): 417.

Demain AL, Fang A. 2000. The Natural Functions of Secondary Metabolites. Adv. Biochem. Engin./Biotechnol., 69: 1-39.

Dhale MA, Vijay-Raj AS. 2009. Pigment and amylase production in Penicillium sp NIOM-02 and its radical scavenging activity. J. Food Sci. Technol., 44(12): 2424-2430.

Gautier M, Normand AC, Ranque S. 2016. Previously unknown species of *Aspergillus*. Clin. Microbiol. Infect., 22(8): 662-669.

Hoffman H, Rice C, Skordalakes E. 2017. Structural Analysis Reveals the Deleterious Effects of Telomerase Mutations in Bone Marrow Failure Syndromes. J Biol Chem., 292: 4593-4601.

Huai Q, Wang H, Liu Y, Kim HY, Toft D, Ke H. 2005. Structures of the N-Terminal and Middle Domains of *E. coli* Hsp90 and Conformation Changes upon ADP Binding. Structure, 13(4): 579-590.

Hunt J, Cheng A, Hoyles A, Jervis E, Morshead CM. 2010. Cyclosporin A Has Direct Effects on Adult Neural Precursor Cells. J. Neurosci., 30(8): 2888-2896.

Jain A, Jain P, Parihar DK. 2020. Antidiabetic and Antibacterial Activity of Non-conventional Curcuma Species. J. Biol. Act. Prod. Nat., 9(6):457-464.

Koganti P, Tulsawani R, Sharma P, Sharma M, Arora S, Misra K. 2018. Role of Hydroalcoholic Extract of Lingzhi or Reishi Medicinal Mushroom, Ganoderma lucidum (Agaricomycetes), in Facilitating Cellular Acclimatization in a Low-Oxygen Microenvironment. Int. J. Med. Mushrooms, 20(5): 431-444.

Li X, Xia Z, Tang J, Wu J, Tong J, Li M, Ju J, Chen H, and Wang L. 2017. Identification and Biological Evaluation of Secondary Metabolites from Marine Derived Fungi-Aspergillus sp. SCSIOW3, Cultivated in the Presence of Epigenetic Modifying Agents, Molecules, 22(8): 1302.

Lin MT, Mahajan JR, Dianese JC, Takatsu A. 1976. High Production of Kojic Acid Crystals by Aspergillus parasiticus UNBF A12 in Liquid Medium. Appl Environ Microbiol., 32(2): 298-299.

Luoto KR, Meng AX, Wasylishen AR, Zhao H, Coackley CL, Penn LZ, Bristow RG. 2010. Tumor Cell Kill by c-MYC Depletion: Role of MYC-Regulated Genes that Control DNA Double-Strand Break Repair. Cancer Res., 70(21): 8748-8759.

Manupati K, Debnath S, Goswami K, Bhoj PS, Chandak HS, Bahekar SP, Das A. 2019. Glutathione S-transferase omega 1 inhibition activates JNK-mediated apoptotic response in breast cancer stem cells. The FEBS Journal, 286(11): 2167-2192.

Manupati K, Dhoke NR, Debnath T, Yeeravalli R, Guguloth K, Saeidpour S, De UC, Debnath S, Das A. 2017. Inhibiting epidermal growth factor receptor signalling potentiates mesenchymal-epithelial transition of breast cancer stem cells and their responsiveness to anticancer drugs. FEBS J., 284(12): 1830-1854.

Maritim AC, Sanders RA, Watkins JB. 2003. Diabetes, oxidative stress, and antioxidants: A review. J. Biochem. Mol. Toxicol., 17(1): 24-38.

Martín JF, Casqueiro J, Liras P. 2005. Secretion systems for secondary metabolites: how producer cells send out messages of intercellular communication. Curr Opin Microbiol., 8(3): 282-293.

Matassov D., Kagan T., Leblanc J., Sikorska M., Zakeri Z. (2004) Measurement of Apoptosis by DNA Fragmentation. In: Brady H.J.M. (eds) Apoptosis Methods and Protocols. Methods in Molecular Biology, vol 282. Humana Press.

Miranda H, Simão R, Dos Santos Vigário P, De Salles BF, Pacheco MTT, Willardson JM. 2010. Exercise order interacts with rest interval during upper-body resistance exercise. J. Strength Cond. Res., 24(6): 1573-1577.

Misra S, Beach BM, Hurley JH. 2000. Structure of the VHS domain of human Tom1 (target of myb 1): insights into interactions with proteins and membranes. Biochemistry, 39(37): 11282-11290.

Naik PK, Santoshi S, Rai A, Joshi HC. 2011. Molecular modelling and competition binding study of Br-noscapine and colchicine provide insight into noscapinoid-tubulin binding site. J. Mol. Graph. Model., 29(7): 947-955.

Nishihara K, Kanemori M, Yanagi H, Yura T. 2000. Overexpression of Trigger Factor Prevents Aggregation of Recombinant Proteins in *Escherichia coli*. Appl. Environ. Microbiol., 66(3): 884.

Niwa Y, Terashima T, Sumi H. 2003. Topical application of the immunosuppressant tacrolimus accelerates carcinogenesis in mouse skin. Br. J. Dermatol., 149(5): 960-967.

Otto J, Ordovas JM, Smith D, van Dongen D, Nicolosi RJ, Schaefer EJ. 1995. Lovastatin inhibits diet induced atherosclerosis in F1B Golden Syrian hamsters. Atherosclerosis, 114(1): 19-28.

Palanichamy P, Krishnamoorthy G, Kannan S, Marudhamuthu M. 2018. Bioactive potential of secondary metabolites derived from medicinal plant endophytes. Egypt. J. Basic Appl. Sci., 5(4): 303-312.

Pandit SG, Puttananjaih MH, Harohally NV, Dhale MA. 2018. Functional attributes of a new molecule-2-hydroxymethyl-benzoic acid 2′-hydroxy-tetradecyl ester isolated from Talaromyces purpureogenus CFRM02Food Chem., 255: 89-96.

Parshikov IA, Woodling KA, Sutherland JB. 2015. Biotransformations of organic compounds mediated by cultures of Aspergillus niger. Appl. Microbiol. Biotechnol., 99(17): 6971-6986.

Roe SM, Ali MMU, Meyer P, Vaughan CK, Panaretou B, Piper PW, Prodromou C, Pearl LH. 2004. The Mechanism of Hsp90 Regulation by the Protein Kinase-Specific Cochaperone p50cdc37. Cell, 116(1): 87-98.

Sahu M, Jha H. 2020. Study on Antioxidant, Antidiabetic and Antibacterial Activity of Rhizospheric Fungi from Achanakmar Biosphere Reserve, Bilaspur. Egypt. J. Microbiol, 55(1): 29-44.

Sahu MK, Kaushik K, Das A, Jha, H. 2020. In vitro and *in silico* antioxidant and antiproliferative activity of rhizospheric fungus Talaromyces purpureogenus isolate-ABRF2. Bioresour. Bioprocess, 7(1): 1-16.

Sarker SD, Nahar L, Kumarasamy Y. 2007. Microtitre plate-based antibacterial assay incorporating resazurin as an indicator of cell growth, and its application in the *in vitro* antibacterial screening of phytochemicals. Methods, 42(4): 321-324.

Satelli A, Li S. 2011. Vimentin in cancer and its potential as a molecular target for cancer therapy. Cell. Mol. Life Sci., 68(18): 3033-3046.

Schulze JM, Kane CM, Ruiz-Manzano A. 2010. The YEATS domain of Taf14 in Saccharomyces cerevisiae has a negative impact on cell growth. Mol. Genet. Genom, 283(4): 365-380.

Sein H, Reinmets K, Peil K, Kristjuhan K, Värv S, Kristjuhan A. 2018. Rpb9-deficient cells are defective in DNA damage response and require histone H3 acetylation for survival. Sci. Rep., 8(1): 1-11.

Sharma D, Pramanik A, Agrawal PK . 2016. Evaluation of bioactive secondary metabolites from endophytic fungus Pestalotiopsis neglecta BAB-5510 isolated from leaves of *Cupressus torulosa* D.Don. 3 Biotech., 6(2): 210.

Shen H.-Y, Jiang HL, Mao HL, Pan G, Zhou L, Cao, YF. 2007. Simultaneous determination of seven phthalates and four parabens in cosmetic products using HPLC-DAD and GC-MS methods. J. Sep. Sci., 30(1): 48-54.

Singh M, Tulsawani R, Koganti P, Chauhan A, Manickam M, Misra K. 2013. Cordyceps sinensis increases hypoxia tolerance by inducing heme oxygenase-1 and metallothionein via Nrf2 activation in human lung epithelial cells. Biomed Res. Int., 2013: 569206.

Soler N, Craescu CT, Gallay J, Frapart YM, Mansuy D, Raynal B, Vernis L. 2012. AS-adenosylmethionine methyltransferase-like domain within the essential, Fe-S-containing yeast protein Dre2. FEBS J., 279(12): 2108-2119.

Sowndhararajan K, Kang SC. 2013. Free radical scavenging activity from different extracts of leaves of Bauhinia vahlii Wight & Arn. Saudi. Sci. J. Biol. Sci., 20(4): 319-325.

Tomar V, Kumar N, Tomar R, Sood D, Dhiman N, Dass SK, Prakash S, Madan J, Chandra R. 2019. Biological Evaluation of Noscapine analogues as Potent and Microtubule-Targeted Anticancer Agents. Sci. Rep., 9(1): 1-11.

VM G. 2010. Focal adhesion kinase as a cancer therapy target. Anticancer Agents Med Chem., 10(10): 735-741.

Wang T, Liu NS, Seet LF, Hong W. 2010. The Emerging Role of VHS Domain-Containing Tom1, Tom1L1 and Tom1L2 in Membrane Trafficking. Traffic, 11(9): 1119-1128.

Wei CL, Huang TS, Fernando SY, Chung KT. 1991. Mutagenecity studies of kojic acid. Toxicol. Lett., 59: 213-220.

Wei SC, Levine JH, Cogdill AP, Zhao Y, Anang NAA, Andrews MC, Allison JP. 2017. Distinct cellular mechanisms underlie anti-CTLA-4 and anti-PD-1 checkpoint blockade. Cell, 170(6): 1120-1133.

Wyatt TT, Wösten HAB, Dijksterhuis J. 2013. Fungal Spores for Dispersion in Space and Time. Adv. Appl. Microbiol., 85: 43-91.

Zhai MM, Li J, Jiang CX, Shi YP, Di DL, Crews P, Wu QX. 2016. The Bioactive Secondary Metabolites from *Talaromyces* species. Nat. Prod. Bioprospect., 6(1): 1-24.

Zhao W, Zheng HZ, Zhou T, Hong XS, Cui HJ, Jiang ZW, Liu XG. 2017. CTT1 overexpression increases the replicative lifespan of MMS-sensitive Saccharomyces cerevisiae deficient in KSP1. Mech. Ageing Dev., 164: 27-36.

Zhou LN, Zhu TJ, Cai SX, Gu QQ, Li DH. 2010. Three New Indole-Containing Diketopiperazine Alkaloids from a Deep-Ocean Sediment Derived Fungus *Penicillium griseofulvum*. Helv. Chim. Acta, 93(9): 1758-1763.

http://www.jbb.uni-plovdiv.bg
DOI: 10.69085/jbb20221001